


RESEARCH ARTICLE

Open Access



Enhancing radiologist's detection: an imaging-based grading system for differentiating Crohn's disease from ulcerative colitis

Ziman Xiong^{1†}, Yan Zhang^{2†}, Peili Wu^{3†}, Jun Chen⁴, Yaqi Shen^{1*} , Ihab Kamel⁵, Xianying Zheng⁶, Bing Wu^{2†} and Zhen Li^{1†}

Abstract

Background Delayed diagnosis of inflammatory bowel disease (IBD) is common, there is still no effective imaging system to distinguish Crohn's Disease (CD) and Ulcerative Colitis (UC) patients.

Methods This multicenter retrospective study included IBD patients at three centers between January 2012 and May 2022. The intestinal and perianal imaging signs were evaluated. Visceral fat information from CT images was extracted, including the ratio of visceral to subcutaneous fat volume (VSR), fat distribution, and attenuation values. The valuable indicators were screened out in the derivation cohort by binary logistic regression and receiver working curve (ROC) analysis to construct an imaging report and data system for IBD (IBD-RADS), which was tested in the validation cohort.

Results The derivation cohort included 606 patients (365 CD, 241 UC), and the validation cohort included 155 patients (97 CD, 58 UC). Asymmetric enhancement (AE) (OR=87.75 [28.69, 268.4]; $P < 0.001$), perianal fistula (OR=4.968 [1.807, 13.66]; $P = 0.002$) and VSR (OR=1.571 [1.087, 2.280]; $P = 0.04$) were independent predictors of CD. VSR improved the efficiency of imaging signs (AUC: 0.929 vs. 0.901; $P < 0.001$), with a threshold greater than 0.97 defined as visceral fat predominance (VFP). In IBD-RADS, AE was the major criterion, VFP and perianal fistula were auxiliary criteria, and intestinal fistula, limited small bowel disease, and skip distribution were special favoring items as their 100% specificity. Grade 3 to 5 correctly classified most CD patients (derivation: 96.5% (352/365), validation: 98.0% (95/97)), and 98% of those were eventually diagnosed with CD (derivation: 97.8% (352/360), validation: 98.0% (95/97)).

Conclusions IBD-RADS can help radiologists distinguish between CD and UC in patients with suspected IBD.

Keywords Inflammatory bowel disease, Crohn's disease, Ulcerative colitis, Visceral fat, Diagnosis, Computed tomography

[†]Ziman Xiong, Yan Zhang and Peili Wu are joint lead authors.

[†]Bing Wu and Zhen Li are joint senior authors.

*Correspondence:

Yaqi Shen

yqshen@hust.edu.cn

Full list of author information is available at the end of the article



Background

Inflammatory bowel disease (IBD) is a recurrent chronic intestinal inflammatory condition, mainly including Crohn's disease (CD) and ulcerative colitis (UC). The worldwide prevalence of IBD continues to rise, affecting an estimated seven million individuals [1]. Diagnosis difficulties, especially in early stages with intermittent symptoms, may lead to underestimation of actual cases. Delayed diagnosis is common, with reports indicating approximately 10% of patients endured gastrointestinal symptoms for at least five years before confirmation [2]. Long-term accumulation of inflammation can cause progressive intestinal damage, thereby elevating the risks of strictures, penetrating lesions, and even malignancy [3]. The association between delayed diagnosis and increased surgery risk has been demonstrated [4]. Moreover, since CD and UC differ in disease behavior and burden, CD patients usually face greater risks of complications and bowel resection, requiring longer hospital stays and higher medical costs [5, 6]. Therefore, timely and accurate diagnosis is crucial, as it could potentially lead to earlier initiation of biologic therapy and halting disease progression.

The diagnosis of IBD currently relies on a comprehensive assessment of the clinical data and various examination results by a multidisciplinary team. However, atypical symptoms, endoscopic limitations, and low histological positive rates reduce the reliability of these results [7–9]. "Endoscopic Skipping," as was previously described, occurs when endoscopy fails to detect proximal small bowel inflammation or inflammation confined to the intestinal wall [8, 10]. A study including 1,471 CD patients found that 8% had ileal active lesions detectable only by computed tomography and magnetic resonance enterography (CTE/MRE), suggesting that imaging severity should be considered when discrepancies exist between radiology and ileoscopy [11]. These findings demonstrate the value of radiological findings in the early detection of IBD. Notably, compared to endoscopic mucosal healing, achieving transmural healing as seen on cross-sectional imaging is increasingly recognized as a more important treatment goal in CD, reflecting a deeper and more comprehensive response to therapy [12]. CTE/MRE is routinely used in current guidelines to assess discontinuous segmental lesions, ulcers, and fistulas, complementing endoscopic and histological findings [13]. In addition to displaying intestinal and extraintestinal lesions, CTE/MRE also provides anatomic information that can be used for body composition analysis [14, 15]. Previous studies have successfully utilized radiological features extracted from visceral adipose tissue (VAT) to distinguish CD from UC [16]. Additionally, VAT quantitative parameters obtained by CTE are related to more

complex behavior and worse prognosis in IBD [15, 17, 18]. Nonetheless, the previous complex analysis, especially in differentiating IBD subtypes, and the lack of interpretation of intestinal lesions in CT images, has hindered the adoption of the aforementioned conclusions in clinical practice.

Currently, established imaging reporting and grading systems, such as LI-RADS for the liver [19], BI-RADS for the breast [20], and PI-RADS for the prostate [21], have significantly enhanced disease recognition and diagnostic interpretation by radiologists. Developing a similar grading system for IBD patients, like IBD-RADS, would further leverage the strengths of cross-sectional imaging in detecting inflammation confined to the intestinal wall, aligning with current diagnostic and therapeutic goals. Additionally, integrating it into clinical workflows would enable radiologists to focus on critical signs and produce more targeted imaging reports for suspected cases. Gastroenterologists would also benefit from standardized reports, enhancing communication among departments and providing crucial evidence, especially in cases with atypical endoscopic results. However, such an approach is lagging in the diagnosis of IBD. Therefore, the purpose of this study was to establish an IBD imaging report and data system (IBD-RADS) for the identification of different subtypes using the information provided by baseline imaging data of IBD patients.

Methods

Ethics statement

The multicenter retrospective study followed the Declaration of Helsinki, analyzed patients with IBD at three hospitals in China (Tongji Hospital of Huazhong University of Science and Technology, West China Hospital of Sichuan University, and the First Affiliated Hospital of Fujian Medical University), and obtained the consent of the ethics committee of each institution, where informed consent was waived due to the anonymity of the data.

Patient cohorts

We collected two patient cohorts, including a derivation cohort for IBD-RADS construction and a subsequent validation cohort. The derivation cohort included IBD patients from three institutions between 2012 and 2021, and the inclusion criteria were: (a) diagnosis of CD or UC determined by a multidisciplinary team based on the latest guidelines at the time; (b) patients underwent CTE scans on admission; (c) age ≥ 18 years old. Patients with incomplete or poor-quality CT images or with history of previous bowel resection were excluded. Newly diagnosed IBD patients between January and May 2022 were included as the validation cohort, and the inclusion and exclusion criteria were consistent with the derivation

cohort. The gender, age, height, weight, baseline laboratory indicators (C-reactive protein (CRP), erythrocyte sedimentation rate (ESR) and serum albumin (Alb)) and the distribution of intestinal lesions based on imaging, endoscopy and histological results were recorded. In a prior study [15], we reported on 316 patients in the current study. The prior report evaluated the discriminative ability of VAT radiomics. The current study included a larger dataset, and proposed a grading system with simplified quantitative parameters.

Image acquisition and evaluation

All CTE scans were performed following the latest imaging protocol [22]. Patient fasted for 4–6 h and avoided gas-producing liquids, then ingested 1000–1500 ml of 2.5% mannitol solution before the scan. After pre-contrast scanning, a contrast-enhanced CT was performed after a rapid bolus of iopromide (Ultravist 370, 370 mg/mL, Bayer Schering Pharma, Berlin, Germany) (1.5 mL/kg) at a rate of 3–5 mL/s, followed by a 20 mL saline flush using a power injector. Images were routinely acquired in the arterial, intestinal, or portal venous phases.

Two radiologists (Z.X. and Y.L., with 4 years of experience) independently evaluated images blinded to the clinical information. Radiologists evaluated the derivation cohort based on their own clinical experience. They assessed active inflammation of the proximal small intestine (including jejunum and proximal ileum), terminal ileum (TI), and colorectum on CTE, using signs such as intestinal wall thickening (≥ 3 mm), mucosal enhancement, intestinal stricture (with or without upstream intestinal dilatation), and intestinal fistula formation [23]. A lesion involving a single segment was defined as single-segmental lesion, whereas lesions involving multiple sites within a single segment or those involving multiple segments were defined as multi-segmental lesions. Active inflammatory regions on CT images that extend continuously along the bowel were defined as continuous lesions, and those distributed in multiple areas with normal segments in between were defined as skip lesions. Moreover, asymmetric enhancement (AE) of the intestinal wall along the mesenteric border, a characteristic finding of CD [23], along with the presence of intestinal fistula, were recorded as “present” or “absent”, with the assessment of AE referencing Figure S1 (Additional file 1: Fig. S1). Given the limited resolution of CT images, patients with suspected IBD at participating institutions have routinely undergone pelvic MRI upon admission to assess for perianal lesions since 2016. Therefore, for patients who have undergone MRI scans, pelvic MRI scans were used to confirm the presence of perianal fistula, characterized by a hyperintensity track on

T2-weighted sequences, regardless of fat suppression, that is connected to the internal orifice of the anorectum [24, 25]. For patients from 2012 to 2015, their perianal fistulas were identified through a combination of CT images, previous perianal surgeries, clinical symptoms, and physical examinations. After finishing the evaluation of the derivation cohort, the two radiologists were trained in radiological diagnosis of IBD and evaluated the validation cohort using the same criteria three weeks later. The results of the two evaluators were compared, and any discrepancies were adjudicated by a senior radiologist (Y.S.), with 13 years of experience.

Image segmentation and fat parameter extraction

Based on a previously developed VAT automatic segmentation algorithm [26, 27], we incorporated new labels including subcutaneous adipose tissue (SAT) and skeletal muscle, obtaining a comprehensive segmentation model, as shown in Fig. 1. To ensure segmentation consistency, arterial-phase CT images of all patients were selected and input into the automated segmentation model, which labels and outputs various components. To minimize heterogeneity from different imaging sources, we normalized both spatial and intensity before feeding the images into the neural network for processing. Although the model has demonstrated high segmentation accuracy in previous studies [27], the output volumes of interest (VOIs) were individually reviewed and manually adjusted to ensure accuracy. The calibrated VOIs were used to extract parameter information. The current study focused only on the segmentation results of VAT and SAT using arterial phase CT images. The fat parameters related to VAT content, distribution and attenuation were calculated using the segmentation results. Due to incomplete SAT scans in obese patients within the pelvic region, we only analyzed the soft tissue in the lumbar region (the upper border of the first lumbar vertebra to the lower border of the fifth lumbar vertebra). The volume ratio of VAT and SAT, denoted as Visceral-to-Subcutaneous Fat Ratio (VSR), can be expressed as:

$$VSR = \frac{\text{Number of SAT pixels}}{\text{Number of VAT pixels}}$$

This formula calculates VSR by dividing the total count of pixels representing VAT by the total count of pixels representing SAT. Additionally, we calculated the VAT area in each slice within the lumbar region, and then calculated the mean, standard deviation (SD),

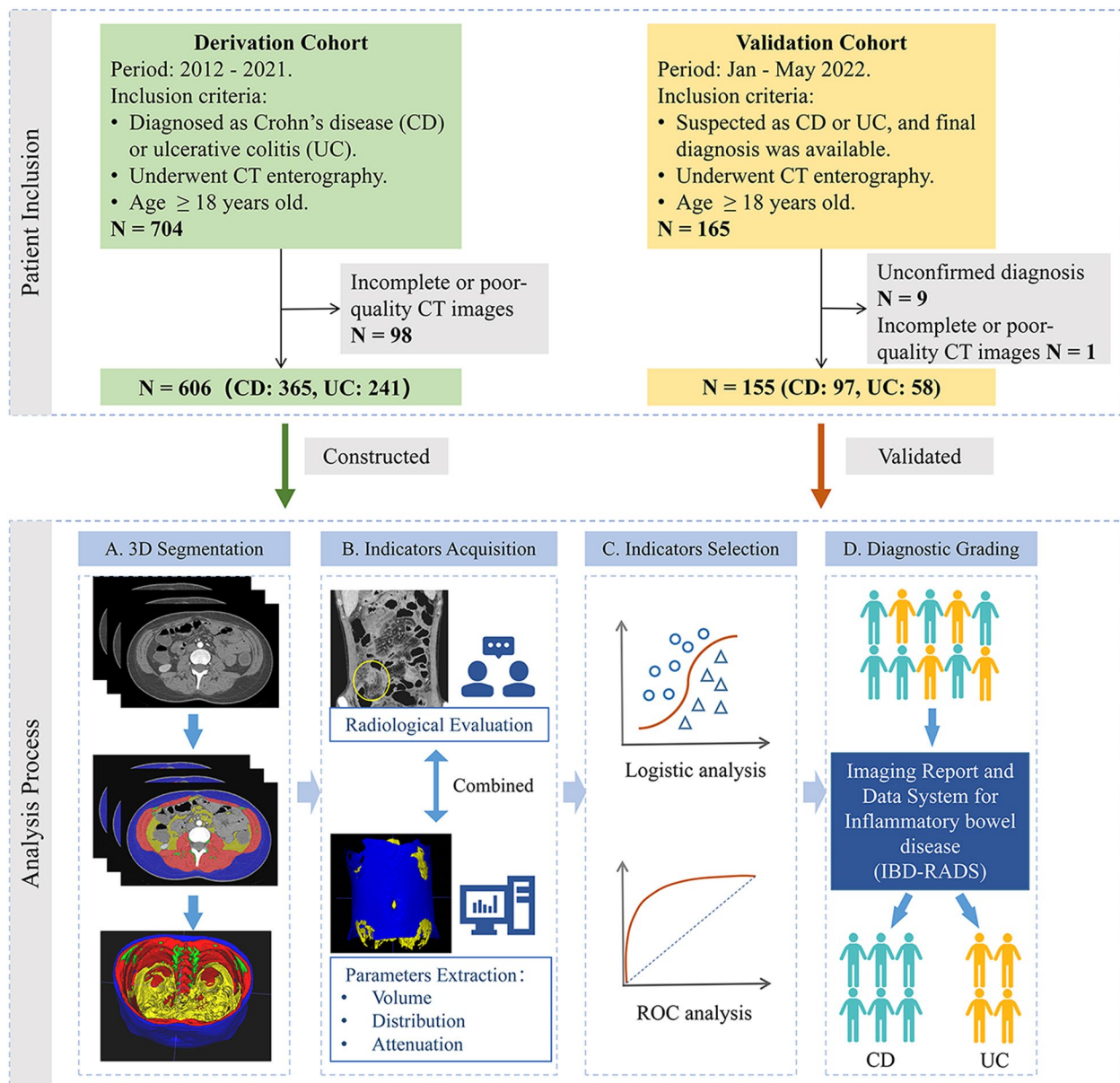


Fig. 1 Overall flowchart of the patient inclusion and analysis process. CD, Crohn’s disease; UC, Ulcerative colitis; ROC, Receiver operating characteristic curves

and coefficient of variation (CV) of areas in the region to reflect the uniformity of VAT distribution. We also extracted CT attenuation values of all VAT pixels in the region and calculated the median, 25% quartile, and 75% quartile.

Statistical analysis

The automatic segmentation and quantitative analysis of fat parameters were performed using Python version 3.7, while the statistical analysis was conducted using SPSS 26.0 and MedCalc Statistical Software version

20.100. Based on the distribution of the data, we used Student’s t-test or Mann–Whitney U test, chi-square test or Fisher’s exact test to compare the differences in various indicators between IBD patients, derivation cohort and validation cohort. Binary logistic regression was used in the derivation cohort to select the predictive factors. Univariate analysis was first performed, and then variables with a $P < 0.05$ were included in the multivariate analysis. Based on the results of above analysis, the diagnostic performance of individual and combined indicators was evaluated using receiver operating characteristic

curves (ROC) and Precision-Recall (PR) curve analysis. The cutoff value of VSR for distinguishing CD from UC was determined using the Youden index in the derivation cohort, and a value above this cutoff indicates that VAT constitutes the majority of the adipose tissue compared to SAT, which is defined as "Visceral Fat Predominance (VFP)." The development of IBD-RADS is based on key indicators identified from the derivation cohort analysis. These indicators were subsequently validated through diagnostic performance analysis in the validation cohort, including ROC and PR curve analysis. The comprehensive integrated discrimination index (IDI) was also calculated. In addition, the consistency of the two radiologists in image evaluation was evaluated by the Kappa coefficient (< 0.4: fair; 0.4–0.6: moderate; 0.6–0.8: substantial; > 0.8: almost perfect). Statistical significance was set at $\alpha=0.05$ (two-sided).

Results

Patient demographic characteristics

Figure 1 shows the inclusion flowchart. We excluded 98 patients with incomplete or poor image quality from 704 patients and eventually enrolled 365 CD and 241 UC patients for the construction of IBD-RADS ($n=606$). For validation, we selected 155 newly diagnosed IBD patients in a subsequent period. Table 1 summarizes the baseline characteristics of all patients. The median age

of CD patients was around 30 years, while that of UC patients was 40 years, consistent in both cohorts. CD patients were predominantly male and had higher levels of inflammatory markers, as well as lower body mass index and Alb levels. In CD patients, the lesions were mainly distributed in the ileocolon (56.2% in derivation and 66.0% in validation) followed by the ileum (27.1% in derivation and 22.7% in validation); while the majority of UC patients had diffuse lesions (53.1% in derivation and 53.4% in validation), followed by left-sided colon lesions (32.4% in derivation and 32.8% in validation). There was no statistical difference in lesion location between the two cohorts ($P=0.20$ and 0.99).

Comparison of radiological results between CD and UC

Comparisons of imaging signs and fat parameters between IBD patients in both cohorts are summarized in Table 2. The differences of imaging signs were consistent in the two cohorts. Although inflammation in the TI was predominantly in CD patients, it was also found in sixty-seven UC patients. Inflammation in the proximal small bowels and lesions confined to small bowels only existed in CD. Lesions in IBD patients were mainly multi-segmental, with CD primarily affecting the ileocolonic region and UC affecting the colon. The lesion distribution of UC patients was continuous, while most CD patients exhibited a skip pattern (76.2% and 82.5%).

Table 1 Baseline characteristics at enrollment of all patients

	Derivation Cohort			Validation Cohort			Comparison ^a	
	CD (n = 365)	UC (n = 241)	P value	CD (n = 97)	UC (n = 58)	P value	P value _{CD}	P value _{UC}
Age (years)	31.0 (25.0, 42.0)	46.0 (34.0, 55.5)	< 0.001*	30.0 (23.0, 35.5)	39.5 (31.8, 53.0)	< 0.001*	0.07	0.22
Gender (Male/Female)	255/110	138/103	< 0.001*	77/20	36/22	0.02*	0.06	0.51
Body mass index (kg/m²)	19.0 ± 2.9 (n = 272)	21.1 ± 3.2 (n = 142)	< 0.001*	19.6 ± 3.2	21.6 ± 3.4	< 0.001*	0.12	0.32
Laboratory findings								
CRP(mg/L)	22.1 (6.4, 55.8)	6.7 (1.8, 21.3)	< 0.001*	24.7 (5.8, 52.6)	4.3 (1.0, 33.1)	0.001*	0.95	0.45
ESR(mm/hr)	27.0 (10.0, 52.0)	16.0 (7.0, 38.0)	< 0.001*	18.0 (9.0, 34.0)	10.5 (4.8, 28.0)	0.014*	0.04*	0.03*
Alb (g/L)	37.9 (32.3, 41.6)	39.7 (34.0, 43.5)	0.003*	38.6 (33.2, 42.5)	41.3 (34.8, 43.8)	0.13	0.58	0.56
Disease location								
CD							0.20	
Ileal	99 (27.1%)	-		22 (22.7%)	-			
Colonic	61 (16.7%)	-		11 (11.3%)	-			
Ileocolonic	205 (56.2%)	-		64 (66.0%)	-			
Upper digestive tract	26 (7.1%)	-		4 (4.1%)	-			
UC								0.99
Ulcerative proctitis	-	35 (14.5%)		-	8 (13.8%)			
Left sided	-	78 (32.4%)		-	19 (32.8%)			
Extensive	-	128 (53.1%)		-	31 (53.4%)			

CD Crohn's disease, UC Ulcerative colitis, CRP C-reactive protein, ESR Erythrocyte sedimentation rate, Alb Serum albumin

* $P < 0.05$ is considered a significant difference

^a Comparison of various indicators between the derivation and the validation cohort

Table 2 Radiological evaluation and analysis of all patients

	Derivation Cohort			Validation Cohort		
	CD (n = 365)	UC (n = 241)	P value	CD (n = 97)	UC (n = 58)	P value
Radiological evaluation						
Involved location						
SB	335 (91.8%)	54 (22.4%)	< 0.001*	93 (95.9%)	13 (22.4%)	< 0.001*
Proximal ^a	160	0		51	0	
Terminal ileum	332	54		93	13	
Colorectum	270 (74.0%)	241 (100%)	< 0.001*	76 (78.4%)	58 (100%)	< 0.001*
Involved segments						
Single	29 (7.9%)	19 (7.9%)	0.98	5 (5.2%)	7 (12.1%)	0.13
SB	26	0	< 0.001*	4	0	0.01*
Colorectum	3	19		1	7	
Multiple	336 (92.1%)	222 (92.1%)	0.98	92 (94.8%)	51 (87.9%)	0.13
SB	69	0	< 0.001*	17	0	< 0.001*
Colorectum	27	168		3	38	
SB + Colorectum	240	54		72	13	
Distribution						
Continuous	87 (23.8%)	241 (100%)	< 0.001*	17 (17.5%)	58 (100%)	< 0.001*
Skip	278 (76.2%)	0 (0.0%)		80 (82.5%)	0 (0.0%)	
Asymmetric enhancement						
Present	287 (78.6%)	8 (3.3%)	< 0.001*	84 (86.6%)	2 (3.4%)	< 0.001*
Absent	78 (21.4%)	233 (96.7%)		13 (13.4%)	56 (96.6%)	
Intestinal fistula						
Present	69 (18.9%)	0 (0.0%)	< 0.001*	16 (16.5%)	0 (0.0%)	0.001*
Absent	296 (81.1%)	241 (100.0%)		81 (83.5%)	58 (100.0%)	
Perianal fistula						
Present	129 (35.3%)	18 (7.5%)	< 0.001*	71 (73.2%)	4 (6.9%)	< 0.001*
Absent	236 (64.7%)	223 (92.5%)		26 (26.8%)	54 (93.1%)	
Fat parameters						
VSR	0.98 (0.58, 1.54)	0.66 (0.42, 1.02)	< 0.001*	0.88 (0.58, 1.34)	0.71 (0.42, 1.00)	0.02*
VAT distribution index						
Mean	38.88 (23.74, 61.31)	46.54 (24.37, 78.62)	0.06	32.43 (16.46, 49.55)	42.17 (22.88, 64.32)	0.06
Standard deviation	9.55 (6.14, 16.10)	9.55 (5.30, 18.81)	0.63	8.21 (4.69, 11.97)	9.73 (6.12, 14.30)	0.08
Coefficient of variation	26.26 (19.21, 35.68)	24.51 (17.38, 32.17)	0.004*	25.14 (22.36, 30.63)	23.67 (21.01, 27.92)	0.07
VAT attenuation index						
Median	-68 (-83.5, -54)	-82 (-96, -68)	< 0.001*	-77 (-90.5, 59.5)	-84.5 (-97.3, -65.8)	0.05
25%	-90 (-102, -77)	-101 (-111.3, -90.8)	< 0.001*	-100 (-110.5, -84)	-104 (-113.5, -91.8)	0.07
75%	-40 (-56, -26.5)	-57 (-73.3, -40.8)	< 0.001*	-46 (-62.5, -32)	-57.5 (-74, -37)	0.02*

CD Crohn's disease, UC Ulcerative colitis, SB Small bowel, VSR Visceral-to-subcutaneous fat ratio, VAT visceral adipose tissue

* $P < 0.05$ is considered a significant difference

^a Proximal small intestine: including jejunum and proximal ileum

The proportion of AE was higher in CD patients, reaching 78.6% (287/365) and 86.6% (84/97) in the derivation and validation cohorts, respectively. Except for twenty

patients with CD and fourteen patients with UC in the derivation cohort, all other patients underwent pelvic MRI scans. Perianal fistula was more common in CD

patients, and intestinal fistula was only observed in CD. For quantitative parameters, CD patients had a greater VSR in both cohorts ($P < 0.001$ and $P = 0.02$); for VAT distribution, although VAT content was lower in CD, their CV was larger ($P = 0.004$ and $P = 0.07$); moreover, the attenuation values in CD were generally higher, especially 75% quartile (< 0.001 and $P = 0.02$).

Screening and validation of diagnostic indicators

Logistic regression analysis included clinical indicators, imaging signs (AE and perianal fistula), and quantitative parameters (VSR, CV and attenuation). Limited small bowel lesions, intestinal fistula, and skip distribution were excluded because they were not observed in UC cases, which prevented model convergence. Multivariate analysis revealed that age, AE, perianal fistula, and VSR were significant predictors of CD (Additional file 2: Table S1). ROC analysis showed that the specificity of limited small bowel lesions, intestinal fistula, and skip distribution reached 100%, and AE also showed good diagnostic performance in distinguishing between CD and UC (area under the curve, AUC, 0.877 [0.848, 0.902]). Perianal fistula (AUC, 0.639 [0.600, 0.678]) and VSR (AUC, 0.657 [0.617, 0.694]) showed similar diagnostic performance ($P = 0.52$), with a VSR cut-off value of 0.97 for defining “VFP”. The clinical indicators of age (AUC, 0.732 [0.695, 0.767]), BMI (AUC, 0.697 [0.650, 0.741]), and CRP (AUC, 0.670 [0.629, 0.709]) also performed well. Details are summarized in Table S2 (Additional file 2: Table S2).

We compared the diagnostic performance of single and combined indicators, as summarized in Table 3. The joint indicator performed better than a single indicator, regardless of the cohort. Figure 2 shows the ROC and PR curves for both cohorts. In the derivation cohort, the AUC of the joint indicator was greater than that of

a single sign ($P < 0.001$), and IDI analysis showed the improvement in discrimination ability. There was no significant difference when AE was combined with perianal fistula or VSR ($P = 0.27$). The combination of AE, perianal fistula and VSR obtained the largest AUC, which was significantly larger than AE + perianal fistula ($P < 0.001$) and AE + VSR ($P = 0.03$). The same trend was also observed in the validation cohort. Additionally, the comparison of AUC among the inflammatory marker CRP, body mass index, and various imaging markers showed that CRP and body mass index were similar to perianal fistula ($P = 0.43$ and 0.21) and VSR ($P = 0.68$ and 0.32), but significantly lower than AE (both $P < 0.001$) and combined imaging markers (both $P < 0.001$).

Construction and validation of IBD-RADS

The IBD-RADS based on the above analysis are summarized in Fig. 3. In IBD-RADS, AE was the major criterion, and perianal fistula and VFP were auxiliary criteria. Limited small bowel disease, intestinal-fistula, and skip distribution were highly specific indicators, favoring the diagnosis of CD in particular. We proposed five grades according to the above indicators, and Fig. 3 shows the grade distribution in IBD patients, as detailed in Table 4. Grade 4 and 5 can be initially diagnosed as CD, with 94.3% (derivation) and 95.8% (validation) of CD patients being classified. Grade 3 met only the major criterion and was likely to be diagnosed with CD (57.1% (8/50) and 50.0% (2/4)), with 2.2% (10/462) of CD patients classified into this category. Grade 1 and 2 did not meet the major criterion. Among them, Grade 1 did not have any imaging signs mentioned above, were less likely to be diagnosed with CD (3.6% (6/167) and 2.5% (1/40)) and preferred UC. Grade 2 met only the auxiliary criteria and also preferred UC. Figure 4 shows imaging and

Table 3 Diagnostic Performance Analysis of Single and Combined Indicators

	AUC [95% CI]	AUPRC [95% CI]	Sensitivity (%)	Specificity (%)	Accuracy (%)	PPV (%)	NPV (%)	IDI (%)
Derivation Cohort								
AE	0.877 [0.848, 0.902]	0.924 [0.892, 0.947]	78.6	96.7	85.8	97.3	74.9	
AE + Perianal fistula	0.901 [0.875, 0.924]	0.946 [0.918, 0.965]	78.6	96.7	86.3	92.2	79.0	2.8
AE + VSR	0.912 [0.887, 0.934]	0.951 [0.923, 0.969]	81.9	95.0	86.6	96.4	76.7	3.4
AE + Perianal fistula + VSR	0.929 [0.905, 0.948]	0.961 [0.936, 0.977]	81.1	95.9	86.8	93.6	78.9	5.6
Validation Cohort								
AE	0.916 [0.860, 0.954]	0.949 [0.883, 0.979]	86.6	96.6	90.3	97.7	81.2	
AE + Perianal fistula	0.962 [0.919, 0.986]	0.981 [0.924, 0.996]	94.9	89.7	92.9	93.9	91.2	9.8
AE + VSR	0.941 [0.891, 0.972]	0.971 [0.911, 0.991]	88.7	96.6	91.0	97.7	82.4	2.3
AE + Perianal fistula + VSR	0.964 [0.922, 0.987]	0.983 [0.925, 0.996]	91.8	96.6	92.9	93.9	91.2	10.2

AUC Area under the curve, AUPRC Area under the precision-recall curve, PPV Positive predictive value, and NPV Negative predictive value, IDI Integrated discrimination improvement, AE Asymmetric enhancement, VSR Visceral-to-subcutaneous fat ratio

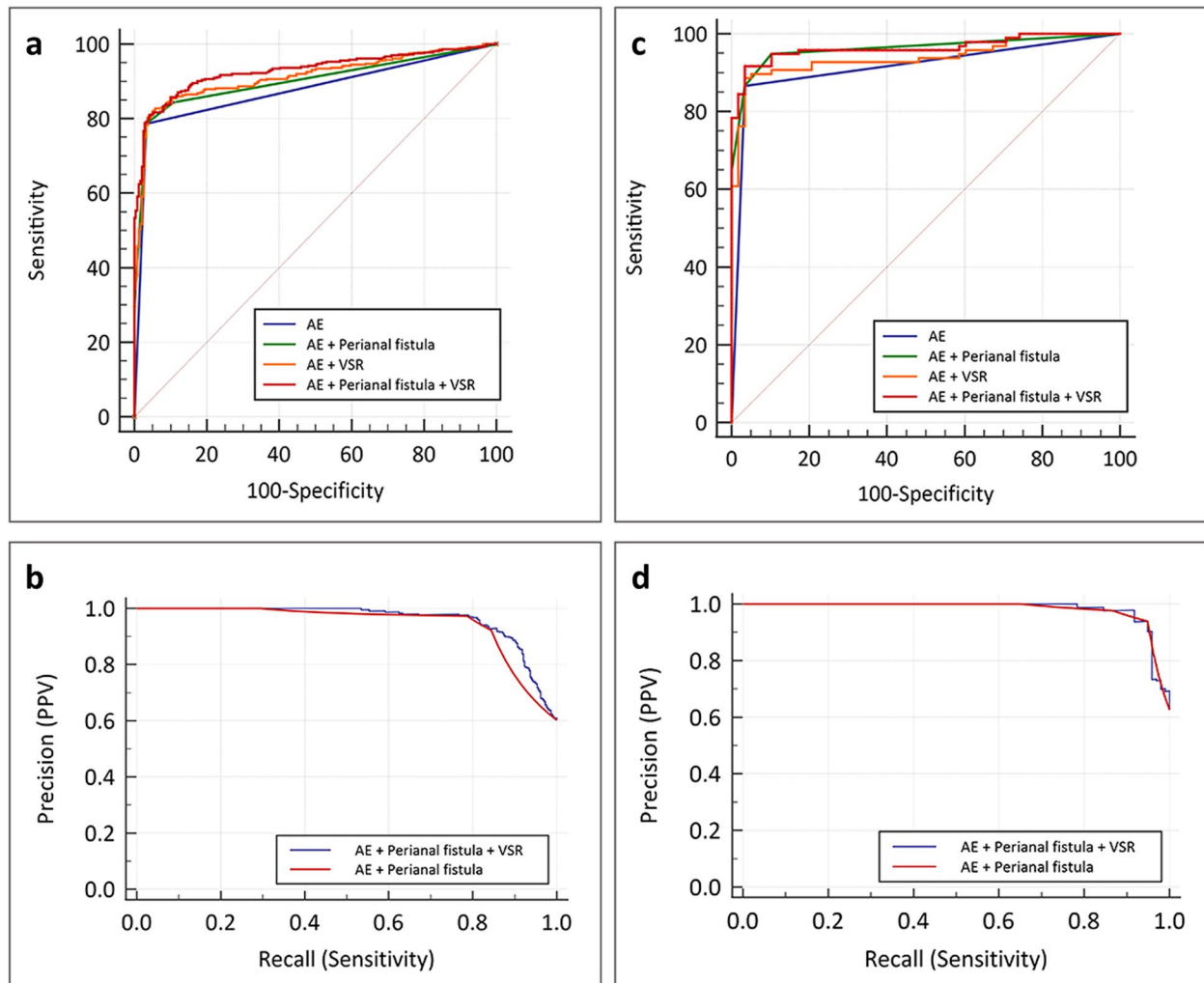


Fig. 2 The Receiver operating characteristic and Precision-Recall curves of derivation and validation cohorts. **a-b** In the derivation cohort, the AUC of AE was 0.877, and no significant difference was observed when AE combined with perianal fistula or VSR (AUC: 0.901 vs. 0.912; $P=0.27$). The combination of three indicators obtained the largest AUC (0.929), significantly larger than AE + perianal fistula (0.901; $P<0.001$) and AE + VSR (0.912; $P=0.03$). The AUPRC of imaging signs combined with VSR was greater than that of combined imaging signs alone (0.961 vs. 0.946). **c-d** In the validation cohort, the AUC of AE was 0.916. The combination of three indicators also obtained the largest AUC (0.964) and AUPRC (0.983 vs. 0.981). AUC, area under the curve; AE, Asymmetric enhancement; VSR, Visceral-to-subcutaneous fat ratio; AUPRC, area under the precision-recall curve

endoscopic images of three patients classified as Grade 5b (a-b) and Grade 1 (c), respectively.

Interobserver reproducibility

The Kappa coefficients for each imaging sign are summarized in Table S3 (Additional file 2: Table S3). Whether in which cohort, the consistency of indicators was between substantial and almost perfect, with the consistency of UC generally higher than that of the CD group. After training, the consistency of the evaluators in assessing the validation cohort significantly improved, as reflected in each item.

Discussion

We identified discriminative imaging features and quantitative parameters from baseline radiological examinations of IBD patients upon admission. Subsequently, an imaging-based grading system, IBD-RADS, specifically designed for CD was constructed and validated. IBD-RADS highlights the importance of radiological findings and the complementary role of quantitative parameters to imaging signs. Notably, Grade 3 to 5 correctly classified most CD patients (derivation: 96.5%, validation: 98.0%), making it valuable for the initial stratification of clinically suspected IBD patients.

IBD-RADS	Definition	
1	Does not meet any of the criteria	Major criterion Asymmetric enhancement of the intestinal wall along the mesentery border Auxiliary criteria Perianal fistula Visceral Fat Predominance Favoring CD in particular Limited small bowel disease Interintestinal fistula Skip distribution
2	Isolated Auxiliary criteria	
3	Isolated Major criterion	
4	a. Major criterion + Auxiliary criteria	
	b. Isolated Favoring signs	
	c. Favoring signs + Auxiliary criteria	
5	a. Major criterion + Favoring signs	
	b. Major criterion + Auxiliary criteria + Favoring signs	

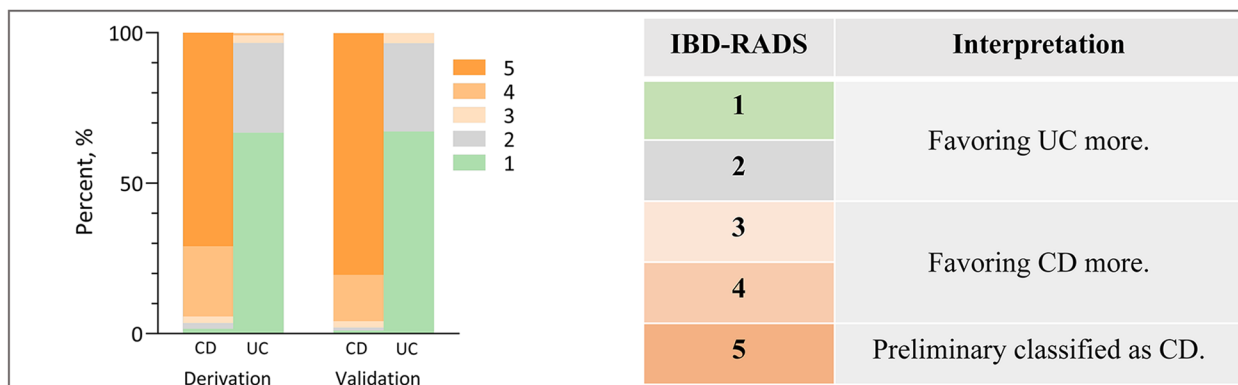


Fig. 3 Criterion, definitions, and interpretations of IBD-RADS, and its distribution in the two cohorts. IBD-RADS includes one major criterion, two auxiliary criteria, and three special support items. The grading system classifies patients into five grades, with Grade 4 and 5 further subdivided into three and two categories, respectively. Based on the distribution in the derivation and validation cohorts, we recommend that Grade 1 and 2 patients should be initially classified as UC, while Grade 3 and 4 are more indicative of CD. Patients classified as Grade 5 can be preliminarily classified as CD. CD, Crohn's disease; UC, Ulcerative colitis

Table 4 Distribution of patients in the Derivation and Validation cohorts

IBD-RADS	Derivation Cohort (n = 606)			Validation Cohort (n = 155)		
	N (%)	CD (n = 365)	UC (n = 241)	N (%)	CD (n = 97)	UC (n = 58)
1	167 (27.6)	6 (1.6)	161 (66.8)	40 (25.8)	1 (1.0)	39 (67.2)
2	79 (13.0)	7 (1.9)	72 (29.8)	18 (11.6)	1 (1.0)	17 (29.3)
3	14 (2.3)	8 (2.2)	6 (2.5)	4 (2.6)	2 (2.1)	2 (3.4)
4	87 (14.4)	20 (5.5)	2 (0.8)	15 (9.7)	4 (4.1)	0
		22 (6.0)	0		3 (3.1)	0
		43 (11.8)	0		8 (8.2)	0
5	259 (42.7)	71 (19.5)	0	78 (50.3)	12 (12.4)	0
		188 (51.5)	0		66 (68.0)	0

IBD-RADS Imaging report and data system for inflammatory bowel disease, CD Crohn's disease, UC Ulcerative colitis

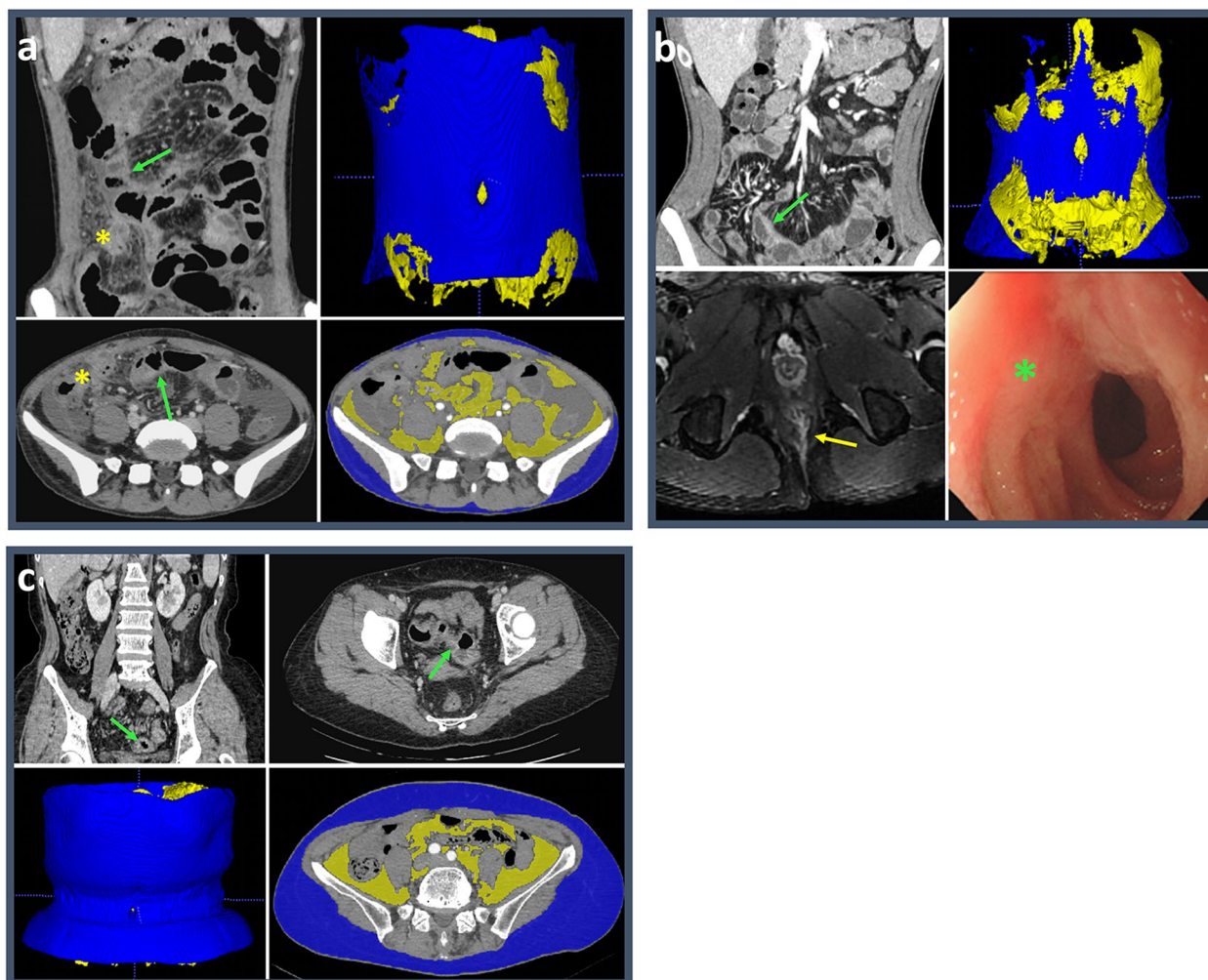


Fig. 4 CTE, pelvic MRI and endoscopic images of two Grade 5 CD patients and one Grade 1 grade UC patient. **a** The CTE images of a 24-year-old male with CD showed asymmetric enhancement (green arrow) and intestinal fistula (yellow asterisk). The visceral and subcutaneous fat were marker as yellow and blue, respectively, and the VSR is 1.19 (>0.97 , visceral fat predominance). He was classified as Grade 5b. **b** The CTE, pelvic MRI and endoscopic images of a 24-year-old male patient with CD showed discontinuous asymmetric enhancement (green arrow), perianal fistula (yellow arrow) and longitudinal ulcer (green asterisk), and the VSR was 2.55 (>0.97 , visceral fat predominance). He was classified as Grade 5b. **c** The CTE image of a 55-year-old female patient with UC showed symmetric enhancement of the sigmoid colon with a VSR of 0.38 (<0.97). She was classified as Grade 1. CTE, CT enterography; CD, Crohn's disease; UC, Ulcerative colitis

The IBD-RADS consists of five imaging signs and one quantitative parameter, with AE of the bowel wall along mesenteric border on CTE images serving as the major criterion due to its high sensitivity and specificity in both cohorts. Longitudinal ulcer along the mesenteric border is a recognized feature of CD, as the mesenteric and antimesenteric borders have different blood supply [28]. The mesenteric border side of TI, a susceptible target for CD, is supplied by short vessels, which act as effective terminal arteries and supply a mucosa more susceptible to ischemia, resulting in preferential ulceration [29]. Imaging signs corresponding to this

feature (asymmetric bowel wall thickening, enhancement, and pseudodiverticula on the antimesenteric side) have been described and considered characteristic of active CD [23]. In this study, we investigated AE, and confirmed that it is a sign that occurs in 80% of CD patients and is one of the independent predictors of CD. In addition, we also found that the presence of isolated small bowel disease, intestinal fistulas, and skip distribution in the CTE images were three favoring items for the diagnosis, occurring only in CD. However, since these signs can occur in non-IBD population, they are not used as major criteria. Favoring items maximize

their diagnostic utility only when major criteria are met, as various infectious diseases and malignancies can lead to similar imaging findings [30, 31].

Previous guidelines have emphasized the importance of perianal lesions for CD diagnosis [13]. In the current study, perianal fistula confirmed by imaging was used as an auxiliary criterion, and its addition significantly improved the diagnostic performance of the major criterion alone. However, CTE only reveals extensive and obvious lesions, while pelvic MRI is the best method for visualizing the anatomy of fistulas, especially in clinically asymptomatic patients [23, 32]. Therefore, we recommend suspected IBD patients receive both CTE and pelvic MRI for initial imaging screening. Another auxiliary criterion is VFP, which means a higher proportion of VAT compared with SAT and significantly improves the diagnostic performance of using major criterion or imaging signs alone. The role of adipose tissue in IBD is constantly being interpreted, and relevant clinical, imaging and cytomolecular studies are gradually confirming that VAT is an endocrine organ that regulates immunity and inflammation rather than just an energy storage tissue [33]. Significant differences in VAT have been observed between patients with CD and UC. In CD patients, increased VAT is often associated with “creeping fat,” where mesenteric fat wraps around inflamed intestinal segments, a phenomenon that is uncommon in UC patients [34]. The presence of creeping fat in CD is linked to intestinal fibrosis and disease progression [35]. SAT levels are primarily linked to nutritional status, whereas VAT accumulation is affected by both nutritional factors and disease processes, underscoring its complex role. The VFP, derived from VSR, which accounts for both VAT and SAT, effectively highlights the critical role of VAT in disease pathology. Previous studies have extracted VAT texture features from CT images to identify IBD subtypes, but manual segmentation and a lack of exploration of intestinal lesions limit their clinical application [16]. Volume-based VSR was also calculated in a study using automatic segmentation, but its predictive ability for CD disease progression is limited [17]. We speculate that this index has greater diagnostic value, as VFP in a single slice has been proven useful in differentiating between CD and intestinal tuberculosis [36–39]. To avoid selection bias, we performed analysis of the entire lumbar region and automated the analysis process including segmentation and parameter extraction. Interestingly, despite lower BMI and poorer nutritional status, CD patients have a higher VAT proportion than UC patients, highlighting the crucial role of VFP in disease diagnosis. It is noteworthy that although the VAT distribution and attenuation parameters did not show

statistical significance in multivariate analysis, the differences between CD and UC patients were not negligible, thus confirming the value of fat parameters in IBD studies.

Although multiple diagnostic indicators were proposed, our analysis showed that using auxiliary criteria alone cannot effectively stratify IBD patients. Maximum diagnostic efficacy can only be achieved by using a multiparametric approach. Additionally, integrating IBD-RADS into current clinical workflows is essential to maximize its effectiveness. Radiologists can use this grading system to initially classify suspected IBD patients, expediting diagnosis by gastroenterologists and enabling earlier treatment planning. A standardized grading system can also enhance communication among various healthcare providers in a multidisciplinary team, including radiologists, gastroenterologists, and surgeons, ensuring that all team members share a common understanding of the disease status. Furthermore, it will facilitate data collection for follow-up and monitoring of patient treatment responses. This allows for the accumulation of standardized data across centers, supporting the continuous improvement of the grading system and uncovering its broader applications. The clinical integration of IBD-RADS requires meeting several conditions, with standardized training for radiologists being the most crucial component. Due to the subjectivity of imaging evaluation, even radiologists with similar levels of experience may differ in their interpretation of findings. Our study results indicate that the consistency of evaluations for all indicators improved among junior radiologists after training. Meanwhile, implementation requires time and resources, such as software updates for automated segmentation models and additional time for system integration into practice. Although an initial investment is necessary, standardized processes can significantly improve diagnostic efficiency and accuracy over the long term. Finally, we suggest establishing a continuous evaluation and feedback mechanism. Regularly updating the grading standards based on the latest research and clinical experience of the multidisciplinary team will help optimize the system's application. However, it is important to note that the imaging-based grading system is a stratification tool rather than a diagnostic standard; it may occasionally produce errors, and when necessary, should be used in conjunction with other assessments, such as endoscopic and pathological findings, to accurately evaluate disease activity.

Our study has several limitations. First, the cross-center study led to inevitable differences in equipment, so we selected indicators with greater consistency and accessibility to establish our grading system. Second, the retrospective design may introduce potential selection

bias, as only patients who met the inclusion criteria and had radiological data were included, which may not represent the overall IBD population. Third, our study focused on the diagnostic value of radiology, and the concordance between IBD-RADS and endoscopy needs to be explored further. Fourth, although clinical indicators were compared, they were only used as a reference to the grading system, and were not our focus, but it is worth investigating in the follow-up research. Fifth, the current IBD-RADS requires further prospective validation, including its application to diverse ethnic groups from various regions and comparison with non-IBD intestinal diseases. Sixth, although the criteria were mainly based on CTE, they are equally applicable to MRE, which is debatable considering that MRE is not the preferred choice for the initial diagnosis. Finally, a comparison between intestinal ultrasound and the IBD-RADS system would provide a more comprehensive perspective for clinical practice. However, due to the limitations of the imaging data obtained in this study, such an analysis could not be conducted and warrants further prospective studies.

Conclusions

In conclusion, we propose a new imaging report and data system for clinically suspected IBD patients, aimed at improving the differentiation between CD and UC. This system utilizes easily assessable, consistent imaging signs and stable quantitative parameters obtained through automated calculations, making it well-suited for clinical application. Future research should focus on prospective validation and refining the grading system to optimize its diagnostic performance and explore its integration into routine clinical workflows.

Abbreviations

AE	Asymmetric enhancement
Alb	Serum albumin
AUC	Area under the curve
CD	Crohn's disease
CRP	C-reactive protein
CTE	Computed tomography enterography
CV	Coefficient of variability
ESR	Erythrocyte sedimentation rate
IBD	Inflammatory bowel disease
MRE	Magnetic resonance enterography
ROC	Receiver operating characteristic curves
SAT	Subcutaneous adipose tissue
SD	Standard deviation
TI	Terminal ileum
UC	Ulcerative colitis
VAT	Visceral adipose tissue
VFA	Visceral fat area
VFP	Visceral fat predominance
VOI	Volume of interest
VSR	Visceral-to-Subcutaneous Fat Ratio

Supplementary Information

The online version contains supplementary material available at <https://doi.org/10.1186/s12916-024-03669-5>.

Supplementary Material 1.

Supplementary Material 2.

Acknowledgements

Not applicable.

Authors' contributions

ZX: Data curation, Formal Analysis, Investigation, Methodology, Visualization, Writing – original draft, Writing – review & editing; YZ: Formal Analysis, Investigation, Validation, Visualization, Writing – original draft, Writing – review & editing; PW: Formal Analysis, Investigation, Validation, Visualization, Writing – original draft, Writing – review & editing; JC: Data curation, Formal Analysis, Writing – review & editing; YS: Conceptualization, Funding acquisition, Project administration, Writing – review & editing; IK: Writing – review & editing; XZ: Resources, Supervision, Writing – review & editing; BW: Resources, Supervision, Writing – review & editing; ZL: Resources, Supervision, Funding acquisition, Project administration, Writing – review & editing. All authors read and approved the final manuscript.

Funding

This work was supported by the grants from National Natural Science Foundation of China (NSFC) No. 82071890 and 62131009.

Availability of data and materials

Code used for automatic segmentation and computation will be made available via GitHub. Data may be made available upon reasonable request and pursuant to appropriate agreements.

Declarations

Ethics approval and consent to participate

This multicenter retrospective study was approved by the Research Ethics Committees from each of the participating centers, and informed consent was waived (approval number: TJ-IRB20210836; TJ-IRB20230890; MRCTA,ECFAH of FMU[2023]297).

Consent for publication

All patients whose images were shown gave their consent for publication.

Competing interests

The authors declare that they have no competing interests.

Additional files description.

Additional File 1: Figure S1 Example of assessing asymmetric enhancement on computed tomography enterography.

Additional File 2: Table S1-S3.

Table S1 Binary logistic regression analysis of variables in the Derivation cohort.

Table S2 Diagnostic analysis of individual indicator in the Derivation cohort.

Table S3 The Kappa coefficients of the radiological evaluation items of the two reviewers.

Author details

¹Department of Radiology, Tongji Hospital, Tongji Medical College, Huazhong University of Science and Technology, Qiaokou District, 1095 Jiefang Avenue, Wuhan, Hubei 430030, China. ²Department of Radiology, West China Hospital, Sichuan University, Guoxue Alley, No. 37, Guoxue Alley, Chengdu, Sichuan 610041, China. ³Department of Radiology, The First Affiliated Hospital of Fujian Medical University, Fuzhou 350005, Fujian, China. ⁴Bayer Healthcare, Wuhan, Hubei 430030, China. ⁵Department of Radiology, University of Colorado Denver Anschutz Medical Campus, Aurora, CO, USA. ⁶Department of Radiology, Fujian Maternity and Child Health Hospital, Fuzhou 350005, Fujian, China.

Received: 19 February 2024 Accepted: 30 September 2024
Published online: 08 October 2024

References

- Alatab S, Sepanlou SG, Ikuta K, Vahedi H, Bisignano C, Safiri S, Sadeghi A, Nixon MR, Abdoli A, Abolhassani H, et al. The global, regional, and national burden of inflammatory bowel disease in 195 countries and territories, 1990–2017: a systematic analysis for the global burden of disease study 2017. *Lancet Gastroenterol Hepatology*. 2020;5(1):17–30.
- Blackwell J, Saxena S, Jayasooriya N, Bottle A, Petersen I, Hotopf M, Alexakis C, Pollok RC. Prevalence and duration of gastrointestinal symptoms before diagnosis of inflammatory bowel disease and predictors of timely specialist review: a population-based study. *J Crohns Colitis*. 2021;15(2):203–11.
- Shah SC, Itzkowitz SH. Colorectal cancer in inflammatory bowel disease: mechanisms and management. *Gastroenterology*. 2022;162(3):715–30.
- Jayasooriya N, Baillie S, Blackwell J, Bottle A, Petersen I, Creech H, Saxena S, Pollok RC. Systematic review with meta-analysis: Time to diagnosis and the impact of delayed diagnosis on clinical outcomes in inflammatory bowel disease. *Aliment Pharm Ther*. 2023;57(6):635–52.
- Frolkis AD, Dykeman J, Negrón ME, DeBruyn J, Jette N, Fiest KM, Frolkis T, Barkema HW, Rioux KP, Panaccione R, et al. Risk of surgery for inflammatory bowel diseases has decreased over time: a systematic review and meta-analysis of population-based studies. *Gastroenterology*. 2013;145(5):996–1006.
- Park KT, Ehrlich OG, Allen JI, Meadows P, Szigethy EM, Henrichsen K, Kim SC, Lawton RC, Murphy SM, Regueiro M, et al. The cost of inflammatory bowel disease: an initiative from the Crohn's & Colitis foundation. *Inflamm Bowel Dis*. 2020;26(1):1–10.
- Sakata T, Niwa Y, Goto H, Hirooka Y, Hayakawa T, Ohmiya N, Kobayashi S. Asymptomatic inflammatory bowel disease with special reference to ulcerative colitis in apparently healthy persons. *AM J GASTROENTEROL*. 2001;96(3):735–9.
- Samuel S, Bruining DH, Loftus EV, Becker B, Fletcher JG, Mandrek JN, Zinsmeister AR, Sandborn WJ. Endoscopic skipping of the distal terminal ileum in Crohn's disease can lead to negative results from ileocolonoscopy. *Clin gastroenterol h*. 2012;10(11):1253–9.
- McHugh JB, Appelman HD, McKenna BJ. The diagnostic value of endoscopic terminal ileum biopsies. *Am J Gastroenterol*. 2007;102(5):1084–9.
- Mansuri I, Fletcher JG, Bruining DH, Kolbe AB, Fidler JL, Samuel S, Tung J. Endoscopic skipping of the terminal ileum in pediatric Crohn's disease. *Am J Roentgenol*. 2017;208(6):W216–24.
- Nehra AK, Sheedy SP, Wells ML, VanBuren WM, Hansel SL, Deepak P, Lee YS, Bruining DH, Fletcher JG. Imaging findings of ileal inflammation at computed tomography and magnetic resonance enterography: what do they mean when ileoscopy and biopsy are negative? *J Crohns Colitis*. 2020;14(4):455–64.
- D'Amico F, Massironi S, Allocca M, Danese S. Advancing transmural remission as a treatment target in Crohn's disease: the future of tight-control strategy? *United Eur Gastroent*. 2023;11(10):948–50.
- Bernstein CN, Eliakim A, Fedail S, Fried M, Geary R, Goh K, Hamid S, Khan AG, Khalif I, Ng SC, et al. World gastroenterology organisation global guidelines inflammatory bowel disease: update august 2015. *J Clin gastroenterol*. 2016;50(10):803–18.
- Weston AD, Korfiatis P, Kline TL, Philbrick KA, Kostandy P, Sakinis T, Sugimoto M, Takahashi N, Erickson BJ. Automated Abdominal Segmentation of CT scans for body composition analysis using deep learning. *Radiology*. 2019;290(3):669–79.
- Bamba S, Inatomi O, Takahashi K, Morita Y, Imai T, Ohno M, Kurihara M, Takebayashi K, Kojima M, Iida H, et al. Assessment of body composition from CT images at the level of the third lumbar vertebra in inflammatory bowel disease. *Inflamm bowel dis*. 2021;27(9):1435–42.
- Zhou Z, Xiong Z, Cheng R, Luo Q, Li Y, Xie Q, Xiao P, Hu D, Hu X, Shen Y, et al. Volumetric visceral fat machine learning phenotype on CT for differential diagnosis of inflammatory bowel disease. *Eur radiol*. 2023;33(3):1862–72.
- Li X, Zhang N, Hu C, Lin Y, Li J, Li Z, Cui E, Shi L, Zhuang X, Li J, et al. CT-based radiomics signature of visceral adipose tissue for prediction of disease progression in patients with Crohn's disease: a multicentre cohort study. *Eclinicalmedicine*. 2023;56: 101805.
- Zhou Z, Xiong Z, Xie Q, Xiao P, Zhang Q, Gu J, Li J, Hu D, Hu X, Shen Y, et al. Computed tomography-based multiple body composition parameters predict outcomes in Crohn's disease. *Insights Imaging*. 2021;12(1):135.
- Chernyak V, Fowler KJ, Kamaya A, Kielar AZ, Elsayes KM, Bashir MR, Kono Y, Do RK, Mitchell DG, Singal AG, et al. Liver Imaging Reporting and Data System (LI-RADS) version 2018: imaging of hepatocellular carcinoma in at-risk patients. *Radiology*. 2018;289(3):816–30.
- Timmers JMH, van Doorne-Nagtegaal HJ, Zonderland HM, van Tinteren H, Visser O, Verbeek ALM, den Heeten GJ, Broeders MJM. The Breast Imaging Reporting and Data System (BI-RADS) in the Dutch breast cancer screening programme: its role as an assessment and stratification tool. *Eur radiol*. 2012;22(8):1717–23.
- Turkbey B, Rosenkrantz AB, Haider MA, Padhani AR, Villeirs G, Macura KJ, Tempny CM, Choyke PL, Cornud F, Margolis DJ, et al. Prostate imaging reporting and data system version 2.1: 2019 update of prostate imaging reporting and data system version 2. *Eur urol*. 2019;76(3):340–51.
- Sturm A, Maaser C, Calabrese E, Annese V, Fiorino G, Kucharzik T, Vavricka SR, Verstockt B, van Rheeën P, Tolan D, et al. ECCO-ESGAR guideline for diagnostic assessment in IBD Part 2: IBD scores and general principles and technical aspects. *J Crohns Colitis*. 2019;13(3):273–84.
- Bruining DH, Zimmermann EM, Loftus EV, Sandborn WJ, Sauer CG, Strong SA. Consensus recommendations for evaluation, interpretation, and utilization of computed tomography and magnetic resonance enterography in patients with small bowel Crohn's disease. *Radiology*. 2018;286(3):776–99.
- Maaser C, Sturm A, Vavricka SR, Kucharzik T, Fiorino G, Annese V, Calabrese E, Baumgart DC, Bettenworth D, Borralho Nunes P, et al. ECCO-ESGAR guideline for diagnostic assessment in IBD Part 1: Initial diagnosis, monitoring of known IBD, detection of complications. *J Crohns Colitis*. 2019;13(2):144–64.
- Sheedy SP, Bruining DH, Dozois EJ, Faubion WA, Fletcher JG. MR imaging of perianal Crohn disease. *Radiology*. 2017;282(3):628–45.
- Li Y, Xiong Z, Jiang Y, Shen Y, Hu X, Hu D, Li Z. Enhancing the differentiation between intestinal Behçet's disease and Crohn's disease through quantitative computed tomography analysis. *Bioengineering (Basel, Switzerland)*. 2023;10(10):1211.
- Xiong Z, Wu P, Zhang Y, Chen J, Shen Y, Kamel I, Wu B, Zheng X, Li Z. Radiological biomarkers reflecting visceral fat distribution help distinguish inflammatory bowel disease subtypes: a multicenter cross-sectional study. *Insights imaging*. 2024;15(1):70.
- Anthony A, Pounder RE, Dhillon AP, Wakefield AJ. Vascular anatomy defines sites of indomethacin induced jejunal ulceration along the mesenteric margin. *Gut*. 1997;41(6):763–70.
- Anthony A, Dhillon AP, Pounder RE, Wakefield AJ. Ulceration of the ileum in Crohn's disease: correlation with vascular anatomy. *J Clin pathol*. 1997;50(12):1013–7.
- Martinolich J, Croasdale DR, Bhakta AS, Ata A, Chismark AD, Valerian BT, Canete JJ, Lee EC. Laparoscopic Surgery for Diverticular Fistulas: Outcomes of 111 consecutive cases at a single institution. *J Gastrointest surg*. 2019;23(5):1015–21.
- Kachaamy T, Weber J, Weitz D, Vashi P, Kundranda M. Successful endoscopic management of a malignant ileovesicular fistula. *Gastrointest endosc*. 2016;84(3):536–7.
- Schwartz DA, Wiersema MJ, Dudiak KM, Fletcher JG, Clain JE, Tremaine WJ, Zinsmeister AR, Norton ID, Boardman LA, Devine RM, et al. A comparison of endoscopic ultrasound, magnetic resonance imaging, and exam under anesthesia for evaluation of Crohn's perianal fistulas. *Gastroenterology*. 2001;121(5):1064–72.
- Eder P, Adler M, Dobrowolska A, Kamhieh-Milz J, Witowski J. The role of adipose tissue in the pathogenesis and therapeutic outcomes of inflammatory bowel disease. *Cells-basel*. 2019;8(6):628.
- Mao R, Doyon G, Gordon IO, Li J, Lin S, Wang J, Le THN, Elias M, Kurada S, Southern B, et al. Activated intestinal muscle cells promote preadipocyte migration: a novel mechanism for creeping fat formation in Crohn's disease. *Gut*. 2022;71(1):55–67.
- Li X, Feng S, Cao Q, Coffey JC, Baker ME, Huang L, Fang Z, Qiu Y, Lu B, Chen Z, et al. Degree of creeping fat assessed by computed tomography enterography is associated with intestinal fibrotic stricture in patients

- with Crohn's disease: a potentially novel mesenteric creeping fat index. *J Crohns Colitis*. 2021;15(7):1161–73.
36. Ko JK, Lee HL, Kim JO, Song SY, Lee KN, Jun DW, Lee OY, Han DS, Yoon BC, Choi HS, et al. Visceral fat as a useful parameter in the differential diagnosis of Crohn's disease and intestinal tuberculosis. *Intest res*. 2014;12(1): 42.
 37. Kedia S, Madhusudhan KS, Sharma R, Bopanna S, Yadav DP, Goyal S, Jain S, Das P, Dattagupta S, Makharia G, et al. Combination of increased visceral fat and long segment involvement: development and validation of an updated imaging marker for differentiating Crohn's disease from intestinal tuberculosis. *J Gastroen hepatol*. 2018;33(6):1234–41.
 38. Yadav DP, Madhusudhan KS, Kedia S, Sharma R, Pratap Mouli V, Bopanna S, Dhingra R, Pradhan R, Goyal S, Sreenivas V, et al. Development and validation of visceral fat quantification as a surrogate marker for differentiation of Crohn's disease and intestinal tuberculosis. *J Gastroen Hepatol*. 2017;32(2):420–6.
 39. Seetharaman J, Srivastava A, Yadav RR, Singh SK, Mishra P, Sen Sarma M, Poddar U. Visceral fat indices: do they help differentiate crohn's disease and intestinal tuberculosis in children? *J Crohn's Colitis*. 2023;17:2026–32.

Publisher's Note

Springer Nature remains neutral with regard to jurisdictional claims in published maps and institutional affiliations.